J. Cosmet. Sci., **62,** 469–482 (September/October 2011)

Diguanoside tetraphosphate (Gp_4G) is an epithelial cell and hair growth regulator

DIVINOMAR SEVERINO, TELMA M.T. ZORN, GUSTAVO A. MICKE, ANA C. O. COSTA, JOSÉ ROBERTO M.C. SILVA, LEANDRO F. NOGUEIRA, ALICA J. KOWALTOWSKI, and MAURÍCIO S. BAPTISTA, *Departamento de Bioquímica, Instituto de Química, Universidade de São Paulo* (*D.S., A.J.K., M.S.B.*), *Instituto de Ciências Biomédicas, Universidade de São Paulo* (*T.M.T.Z., J.R.M.C.S.*), *Universidade Federal de Santa Catarina* (*G.A.M.*), *Departamento de Química Fundamental, Instituto de Química, Universidade de São Paulo* (*A.C.O.C.*), *and Universidade Estadual de Mato Grosso* (*L.F.N.*), *Brazil.*

Accepted for publication June 7, 2011.

Synopsis

Our goal was to study the effect of Gp_4G on skin tissues and unravel its intracellular action mechanisms. The effects of Gp_4G formulation, a liposomic solution of *Artemia salina* extract, on several epidermal, depmal, and hair follicle structures were quantified. A 50% increase in hair length and a 30% increase in the number of papilla cells were explained by the changes in the telogen/anagen hair follicle phases. Increasing skin blood vessels and fibroblast activation modified collagen arrangement in dermal tissues. Imunohistochemical staining revealed expressive increases of versican (VER) deposition in the treated animals (68%). Hela and fibroblast cells were used as *in vitro* models. Gp_4G enters both cell lines, with a hyperbolic saturation profile inducing an increase in the viabilities of Hela and fibroblast cells. Intracellular ATP and other nucleotides were quantified in Hela cells showing a 38% increase in intracellular ATP concentration and increases in the intracellular concentration of tri- , di- , and monophosphate nucleosides, changing the usual quasi-equilibrium state of nucleotide concentrations. We propose that this change in nucleotide equilibrium affects several biochemical pathways and explains the cell and tissue activations observed experimentally.

INTRODUCTION

Hair growth and loss in mammalian species is controlled by a specific follicular cell cycle that includes periods of growth (anagen phase), regression (catagen phase), and rest (telogen phase) (1,2). In the earlier stages of the anagen phase, dermal papillae are restimulated to produce new hair shafts. Matrix bulb cells die by apoptosis in the catagen phase, and follicles remain in a resting state in the telogen phase until signaling factors activate them.

Address all correspondence to Maurício S. Baptista at baptista@iq.usp.br.

Understanding this cycle is highly important to control hair loss, and several authors have published comprehensive articles on this subject (3–6). Several drugs interfere with different steps of the follicle cycle, affecting hair growth, stimulating vascularization and cell proliferation, and providing energy resources for the follicles. However, there are few studies aiming to detect the effects of bioextracts that facilitate hair elongation (7). The indirect effects of antioxidants, which bring general benefits to skin health, have been shown to improve hair growth (7).

Apoptosis has also been shown to allow a shift from anagen to catagen phases in the follicle cycle (2,3,8). Apoptosis can be initiated by the activation of death domain receptors, present in the intracellular domain of the TGF-β receptor. Antagonists of TGF-β cause delays in the outcome of the catagen phase and consequent extension of the anagen phase, which can elongate the life cycle of a hair shaft (3,8). Some plant extracts have also been shown to suppress TGF-β2 (9). Interesting initial results suggest that adenosine can promote hair growth through the activation of specific receptors in the follicular bulb, increasing the release of fibroblast growth factor 7, which activates hair growth (10).

Topical applications of minoxidil were widely used to induce hair growth, desite its collateral effects (11). Although its action mechanism has been thoroughly studied, it is not yet totally understood. Minoxidil is known to be a nitric oxide (NO) agonist promoting opening of K^+ channels and vasodilatation. Such actions may increase follicular irrigation, facilitating oxidative metabolism in the follicles (5,11,12).

Hair follicles are highly active structures distinguished by intense cell proliferation and protein synthesis, required during the long period of hair growth. Adequate function of the follicle cycle uses large amounts of intracellular ATP and, consequently, efficient ATP synthesis is required. Therefore, the bioenergetics of bulb cells, as well as the correct homeostasis of dermal tissues, is fundamental to allow cycles of hair growth and involution (4,5). ATP levels can be decreased by a relative depletion of oxygen and/or nutrients in the follicle cells, fibroblasts, and keratinocytes, causing hair loss.

Diguanoside tetraphosphate (Gp_4G) is a symmetrical bis-diphospho nucleoside (Scheme 1) that is found in large concentrations in the cysts of *Artemia salina* (CAS). Finamore and Warner have shown that after the contact of CAS with water, Gp_4G is enzymatically hydrolyzed and increases intracellular ATP around 30 minutes after rehydration (12,13). Small rates of Gp_4G hydrolysis provide a free energy flow and allow the encysted embryos to survive for several years of continuous harsh conditions, including continuous anoxia and hydrolytic stress (14). A similar molecule, which is widely found in mammalian cells, diadenosine tetraphosphate, has been shown to be a pleiotypic activator because its concentration is highly correlated with tissue activity (15).

The increase in intracellular ATP concentrations after Gp_4G hydrolysis has been claimed to cause a stimulating effect that could be helpful in several cosmetic industry

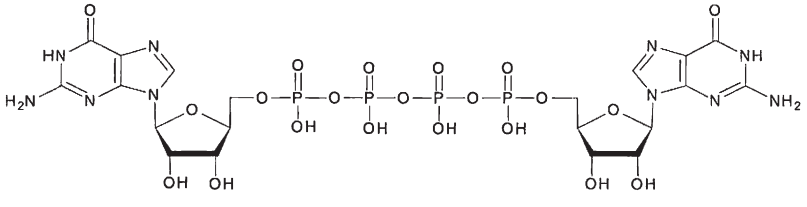

Scheme 1. Molecular of p^1, p^4 diguanoside 5′ tetraphosphate (Gp_4G).

applications, including anti-aging and skin repair (16,17). Although Gp_4G has been on the market for several years, its action mechanisms are unknown. Moreover, there is no published data showing how Gp_4G works on skin components and its effects on the follicle cycle. Therefore, the aim of this work is: (i) to analyze whether the Gp_4G formulation stimulates hair growth; (ii), to characterize morphophysiological parameters in the dermal tissues, and (iii) to propose a biochemical mechanism for its effect.

MATERIALS AND METHODS

Gp_4G FORMULATION

Gp_4G was extracted from CAS by FarmaService Bioextract in São Paulo, Brazil, using a traditional method (14), and its concentration was checked by an adapted capillary electrophoresis method (18,19). Gp_4G extracted from CAS stock solution was used either as a pure solution prepared in MilliQ-water in cell culture studies or as a Gp_4G formulation to enhance skin penetration in *in vivo* experiments, which consisted of a phospholipid vesicle suspension supplemented with calcium and red pepper extract containing 0.69 g/l of gallic acid equivalents in total polyphenols and 1.70 g/l of Trolox equivalent in an antioxidant capacity (DPPH suppression) measured according to the specified literature (18–21). Soybean lecithin was dissolved in a volatile organic solvent, which was evaporated under argon flux and rehydrated with Gp_4G stock solution and calcium chloride 1.0 mM, and finally sonicated for five minutes. The final concentration of lecithin was 2 mg/ml. A control group containing only Gp_4G and liposomes was also implemented, showing results similar to those reported for the Gp_4G formulation, but in smaller magnitude. We suspect that this is due to the fact that both red pepper and calcium are important in allowing better penetration of Gp_4G in the skin.

IN VIVO HAIR ELONGATION EVALUATION

The Gp_4G formulation was topically applied to the dorsal region (8 cm^2, shaved) of Wistar rats (n = 5). The control group was not treated with the product (n = 5). Male rats were born and kept in the Animal Care Facility of the Chemistry Institute of the University of São Paulo. All rats were of the same age (20 days). Therefore, their follicles were in the first telogen phase, and experiments were followed during a hair follicle cycle induced by depilation (22). About 1 ml of the product was applied daily with a cotton swab over a period of 28 days. At the end of the application period, a sample of hair shaft from the treated skin was collected to measure its width. Hair shafts were measured for each animal using a calibrated ruler under a microscope. The distribution of overcoat and undercoat hair shafts was about 70% and 30%, respectively. These two classes were considered together to calculate a general average size and separately to determine the average length of the independent populations of the hair shafts. The experiment was repeated twice.

HISTOLOGICAL STUDIES

Results were analyzed qualitatively and quantitatively after morphometric evaluation in comparison with the control group. At the end of the application period the rats were anesthetized to obtain dorsal skin samples that were immediately fixed properly for histological and immunohistochemical analyses. National standards for the care and use of

laboratory animals, compatible with NIH standards, were followed. All studies were approved by the Institutional Animal Care and Use Committee.

LIGHT MICROSCOPY PROCESSING

Samples were fixed for three hours in Methacarn (methanol; chloroform; glacial acetic acid; 6:3:1), rinsed with absolute ethanol, and embedded in Paraplast (Oxford, St. Louis, MO) at 60°C. Tissues were cut on a microtome (Micron HM-200) into 5-μm sections, affixed to glass slides using 0.1% poly-L-lysine (Sigma, St. Louis, MO), and then dried at room temperature. For morphological analysis, all sections were stained with hematoxylin-eosin. Some sections were histochemically stained by the picrosirius method for evaluation of collagen fiber content and distribution. The observations were performed in a minimum of three sections.

ANAGEN/TELOGEN PHASE DISTINCTION

The phases of the hair cycle were analyzed at the level of the sebaceous gland. Telogen and anagen hair follicle phases were identified in hematoxylin-eosin–stained histological sections and were classified according to Headington (24). This method provides a simple and reliable way to differentiate hair follicles in anagen and telogen. Accordingly, the medulla of the telogen hair follicles were stained in pink by H&E in the region of the sebaceous glands, and the medulla of anagen hair follicles were not stained in pink at the height of the sebaceous glands (24).

IMMUNOPEROXIDASE PROCEDURES

Five-micrometer-thick sections were affixed to glass slides using 0.1% poly-L-lysine (Sigma) and then dried at room temperature. Each of the succeeding steps was followed by thorough rinsing with phosphate-buffered saline (PBS). Sections were treated with 3% H_2O_2 in PBS for 30 min to block endogenous peroxidase activity. All steps were performed in a humidified chamber, and care was taken to avoid the drying out of sections. Antigen retrieval was done by enzymatic treatment of sections before the immunoreaction. For versican immunoreaction, sections were incubated (1 h at 37°C) in 20 mM Tris-HCl, pH 6.0, containing 0.2 U/ml of chondroitinase ABC (Seikagaku Corp., Tokyo, Japan). For laminin immunostaining, sections were incubated with a 2 mg/ml solution of porcine pepsin (1,120 units/mg protein) (Sigma) in pH 2.2 acid buffer for 20 min at room temperature. Nonspecific staining was blocked by incubating the sections (1 hr) with normal goat serum, diluted 1:1 (v/v) in PBS-10% BSA (w/v) (room temperature).

The sections were then incubated with rabbit anti-VER polyclonal antibody (Chemicon International, Temecula, CA) diluted 1:500 in PBS-0.3% (v/v) Tween 20 or with rabbit polyclonal antibody against laminin (BioGenex, CA) diluted 1:50 in PBS-0.3% (v/v) Tween 20. After rinsing in PBS, all sections were incubated with biotin-conjugated secondary antibody (goat anti-rabbit IgG) diluted in PBS for one hour at room temperature (25°C). Subsequently, sections were incubated with the streptavidin/peroxidase complex (Vector Laboratories, Burlingame, CA) for one hour at room temperature. Peroxidase was visualized using 0.03% 3,3′-diaminobenzidine in PBS with 0.03% H_2O_2. To achieve standardization of the immunoreactions for each antibody, the slides from the control and

experimental groups were simultaneously incubated with DAB, and the reaction was immediately interrupted with PBS after a specific period (1–5 min, depending on the antibody). After immunostaining, the sections were counterstained with Mayer's hematoxylin (Merck, Darmstadt, Germany). For each immunoreaction, the negative control was performed by replacing the primary antibodies with the respective non-immune serum at similar concentrations or by omitting the primary antibody step from the protocol. Sections were examined with a Nikon Eclipse E600 microscope. Images were captured using a digital camera (COOL SNAP-PROcf color) and Image-Pro Plus software (Media Cybernetics, Silver Spring, MD).

IN VITRO CELL PROLIFERATION, VIABILITY, AND METABOLISM OF Gp_4G

Hela and primary fibroblasts from Swiss mouse embryos were grown in DMEM containing 100 mg/ml of streptomycin and 100 UI/ml of penicillin at 37°C, in a humid atmosphere with 5% CO_2. The cell uptake of Gp_4G and the viability assays were conducted with extract from CAS (from FarmaService BioExtract) and with Gp_4G acquired from Sigma-Aldrich. Only the results from the CAS extract are shown in the text, although the results obtained were basically the same. Gp_4G from both sources were dissolved in DMEM at 5–10 ppm concentrations and sterilized by 0.22-μm filters to incubate the cells. Cell viability assays were conducted by trypan blue uptake and MTT (3-(4,5-dimethylthiazol-2-yl)-2,5-diphenyltetrazolium). Only cells with more than 90% viability were used in all experiments. After three hours of incubation, MTT assays were used according to the literature, in order to measure the cell viability. Briefly, cells were incubated with 2 mg/ml MTT in PBS for two hours. DMSO was used to dissolve the formazan, and light absorption at 550 nm was read in a Shimadzu UV3901-PC spectrophotometer or in a Tecan-Infinite M200 reader plate. For the colony growth assay, Hela cells were grown in six-well plates with 1000 cells/well over eight days. After most colonies reached more than 10^5 cells, they were counted, fixed with 10% formic aldehyde, and stained with 1.0% violet crystal.

The experiment for determination of ATP concentrations was conducted using bioluminescence and a luciferin-luciferase assay and expressed in 10^5 cells, which were counted using the classical hematocytometer technique (25). Other nucleotides were measured in six-well plates with 1×10^6 cells/well. Cells with Gp_4G at 5 ppm and the control cells were incubated for three hours. After that, the media was removed and 1 ml of 0.8 M $HClO_4$ was added (chemical lysing and mechanically detaching the cells) to denature all enzymes, thus interrupting all enzymatically catalyzed reactions that consume or produce ATP, besides all others that could affect nucleotide concentrations. After 15 minutes over ice, 1 ml of KOH at 0.8 M in aqueous solution was added. The supernatant was carefully removed and transferred to a Millipore filtration unit for exclusion of molecules larger than 5 kDa by centrifugation at 12,000*g* and 4°C. Finally, 20 μl of the filtered samples (containing the nucleotides) was either submitted to the bioluminescent assay or injected in a Shimadzu 20A HPLC system. A column of anionic exchange, Shimadzu WAX-IT (0.46×5 cm), was used in a linear gradient flow of 1 ml/min, starting with 20 mM of phosphate buffer at pH 7.0, and changed after 30 minutes to a 480 mM phosphate buffer at pH 6.0. External standards for ADP, AMP, GTP, GDP, GMP, and Gp_4G were used to identify and quantify the concentrations of all these nucleotides in the cell extracts. A biological triplicate for experiment and control was used to calculate the average and standard deviation (error bars in the graphs).

RESULTS AND DISCUSSION

HAIR GROWTH AND SHIFT IN THE FOLLICLE CYCLE

The first experimental evidence that the Gp_4G formulation favors hair growth was obtained by comparing the size of hair shafts of Wistar rats that were (experiment) or were not (control) treated with the Gp_4G formulation for an average of four weeks, during a hair follicle cycle induced by depilation. The experiment was repeated twice on a total of 20 animals. Hair shafts were on the average 20 ± 2% longer (Figure 1a). Rats have two basic types of hair: guard or overcoat, which can be further sub-grouped into *monotrichs*, *awl,* and *auchenes* and undercoat hairs, which are also called *zigzags*. Separating the hair into two size classes, i.e., above 10 cm (overcoat hairs) and below 6 cm (mostly undercoat hairs), we observed that there was an increase in the size of both undercoat (12 ± 5%) and overcoat (27 ± 2%) hair shafts (Figure 1b,c). However, the increase observed in the undercoat shafts was smaller than the increase observed in the overcoat shafts and was not statistically significant. The most conspicuous effect of the Gp_4G formulation was observed in the overcoat shafts, which may be the first indication of a possible shift in the hair cycle. By counting papillar cells in the bulb of ten follicles in each section for a total of three sections, we were also able to show an average increase in the papillar cell count (32 ± 4%) in the bulbs of the treated follicles (Figure 1d). Therefore, the follicles are somehow being stimulated to induce hair growth. Similar effects have been shown to occur in Wistar rats treated with *Hibiscus rosa-sinensis* extracts. The action mechanism of *Hibiscus* seems to be related to the effect of β-catenin, which prolongs the anagen phase and/or shortens the telogen phase (7,12). Recent results indicate that a seed extract of *Hibiscus abelmoschus* favors FGF-2 activity, which may also help to explain the result cited above (23).

In order to understand the effect of Gp_4G in hair follicles, histological follicles that were either in anagen or telogen phases were counted (Figure 2) (24,26). This method is based on the fact that the medulla of telogen follicles receives a different staining in longitudinal sections at the height of the sebaceous glands (see Methods section). Treatment with Gp_4G formulation causes a decrease in the number of telogen follicles and an increase in the number of anagen follicles when compared with the control group. This provides strong evidence that the average increase in the hair length was promoted by a shift in the hair cycle, either by an expansion in the anagen phase or a shortening of the telogen phase. In terms of potential application to humans, we do not expect to see an increase in

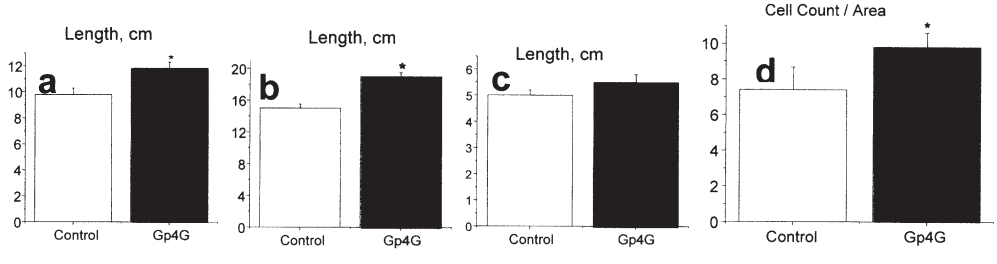

Figure 1. Effect of Gp_4G formulation treatment on the hair follicle structure. (a) Average length of hair shafts, length of (b) undercoat and (c) overcoat hair shafts, and (d) papillar cell count in the bulb of follicles. Cell count represents an average number for all types of follicles. Significantly different from controls, $^*p < 0.05$.

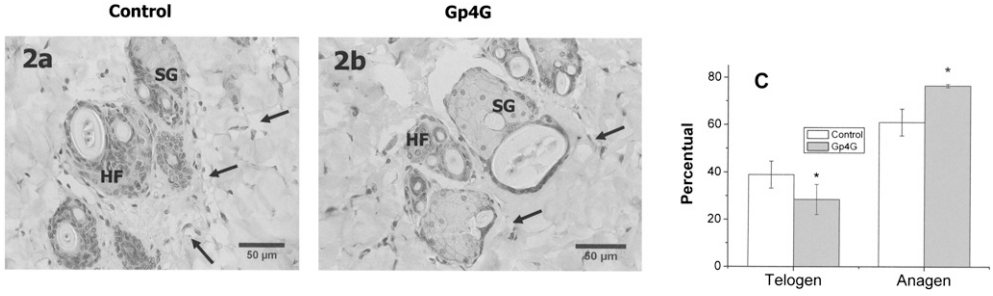

Figure 2. Effect of Gp_4G formulation on the hair growth phases. Sections of H&E-stained dorsal skin from (a) controls (not treated with Gp_4G) and (b) rats treated with Gp_4G formulation. (c) Percentage of anagen and telogen hair growth phases. *Significantly different from controls, $p < 0.001$. Arrows indicate the position of the sections in the height of the sebaceous glands.

facial hair growth since the physiological responses present in human scalp are opposite to those found in facial hair (27).

The fact that the Gp_4G formulation stimulates follicles suggests that it may also be stimulating adjacent interfollicular and bulge stem cells, which may affect the health of dermal and epidermal tissues (28–30). D. Oh and co-workers (27) have shown that even whole proteins (human growth hormone) encapsulated in liposomes, which are delivered to the hair follicles and allowed to interact with their adjacent stem cells, have shown dramatic and generic effects as hair growth, anti-acne effects, skin tone improvement, and anti-wrinkle effects (27,31). To characterize possible actions of the Gp_4G formulation on dermal tissues, we have investigated some key morphofunctional parameters such as vascularization, fibroblast activation, and deposition of collagen and proteoglycan versican in the dermis (32).

EFFECT ON THE DERMIS

Again using Wistar rats that were or were not treated with the Gp_4G formulation, tissue samples were taken and evaluated histologically. The number of active fibroblasts (large cells with irregularly branched cytoplasm) was counted in histological hematoxylin-eosin–stained sections of the skin (Figure 3) (26), and it is clearly higher in the Gp_4G formulation-treated group compared with the control group. It is expected that a higher number of active fibroblasts leads to increased synthesis and deposition of collagen molecules. In fact, the sections stained using the picrosirius method (33), and analyzed using polarized light microscopy, showed a statistically different higher number of thin brilliant green collagen fibrils in skin treated with the Gp_4G formulation, whereas in non-treated skin thick yellow brilliant fibrils were predominant (Figure 4). The high proportion of thin fibers supports our hypothesis that the Gp_4G formulation may favor fibroblast activation and *de novo* synthesis of collagen fibrils in the dermis.

Vascularization is another important parameter that can be related to hair growth and the physiological conditions of epidermal tissues. Figure 5 shows sections of skin immunostained with an anti-laminin (LM) antibody. LM is a specific marker for basement membranes, present in all types of blood vessels (34,35). Importantly, the number of vessels per unit of area showed an expressive increase (38%) in the group treated with the Gp_4G formulation (Figure 5). It has been shown earlier that follicle cycling is associated with

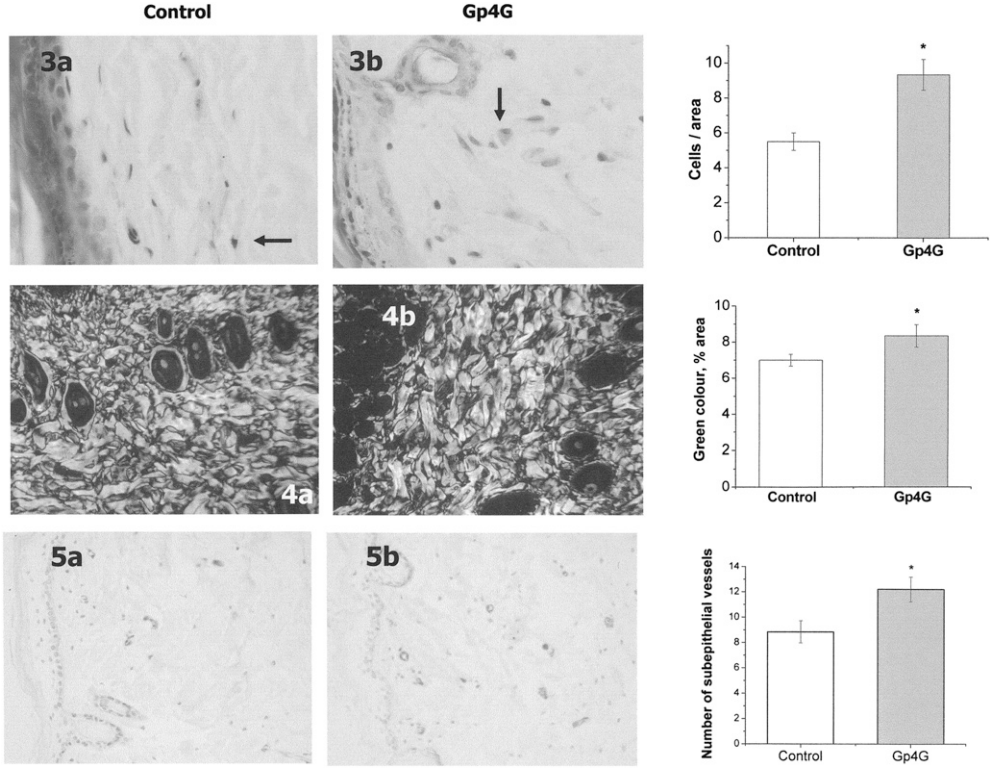

Figure 3. Effect of Gp_4G formulation treatment on the active fibroblasts. H&E-stained paraffin sections showing the higher number of fibroblasts in the (a) Gp_4G-treated skin compared with the (b) non-treated skin. Arrows show examples of active fibroblasts.

Figure 4. Picrosirius-stained sections observed under polarized microscopy. Untreated skin contains predominantly red collagen fibers (a). Thin green and yellow fibers predominate in Gp_4G-treated skin (b). Quantitative evaluation of thin brilliant green and yellow fibers in a section of Gp_4G formulation-treated and untreated skin. Quantifications were conducted by elimination of the specific color channels (blue and red) after *Image J* treatment. *Significantly different from controls, $p < 0.001$.

Figure 5. Effect of Gp_4G formulation treatment on the vascularization of dermal tissues. Average density of subepithelial dermal vessel immunostained with anti-laminin antibody in the (a) Gp_4G formulation-treated and (b) untreated skin. (c) Density of vessels/area in skin section in the subepidermal and deep dermis. *Significantly different from controls, $p < 0.005$.

expressive changes in skin perfusion and that the onset of anagen itself is associated with angiogenisis. We have shown that treatment with the Gp_4G formulation favors both anagen follicles and angiogenisis. Based on our data, we cannot affirm whether the effect of angiogesis is a direct effect of the Gp_4G formulation or is an indirect effect because of the presence of a higher percentage of anagen follicles. However, the fact that both effects were observed experimentally gives confidence that our experimentally gives confidence that our experimental data is self-consistent.

Although the data shown in Figures 2–5 gives a strong indication that the Gp_4G formulation provides direct benefits to the dermal tissue, it was important to test the presence of a recognized marker of cellular proliferation. Versican (VER) is a large chondroitin sulfate proteoglycan that belongs to the family of hyaluronan-binding proteoglycans,

known to play key roles in many cellular signaling pathways involved in hair follicle biology. Previous studies showed that VER is capable of blocking the interaction between cells and other ECM molecules, such as collagen I, fibronectin, and laminin. Pericellular matrix expansion also requires interactions among VER, hyaluronan, and CD44 (36,37). This macromolecular complex increases the viscoelastic nature of the pericellular matrix, creating a highly malleable extracellular environment that controls cell shape, a necessary step for cell proliferation, migration, and histogenesis (38–42).

As expected, VER is expressed in larger amounts in tissues undergoing rapid development or remodeling (42,43). Previous studies have shown that during embryogenesis, a short fragment (839 bp) of human VER is sufficient to promote hair follicle formation (44). In fact, involvement of chondroitin sulfate proteoglycans, such as VER, in hair follicle development and/or hair growth has been suggested because of their dermal papilla (DP)-specific localization in anagenic hair follicles (32). Although the functional roles of VER in hair follicle development and hair growth is not completely understood, several researchers have suggested that VER functions as an inhibitor of cell–cell or cell–extracellular matrix adhesion, allowing DP-cell aggregation (45,46).

In the present study, VER was highly expressed in the matrix and in the cytoplasm of dermal papillar cells (Figure 6) that are in the anagen phase, confirming previous results (32,38). Ten follicles of all subtypes were imaged, and the staining was quantified in each section. Importantly, the immunostaining for VER in the Gp_4G–treated group was 78% higher than in the control (Figure 6c). The anagen phase of the hair follicle is characterized by intense proliferation of both connective tissue cells and papillar cells (5,29,38). As indicated above, the cell proliferation, which is indicative of anagen, is accompanied by increasing expression of VER that signals quiescent papillar cells to restart a new growth cycle (29,38). Accordingly, increasing VER expression in the Gp_4G formulation-treated group indicates that Gp_4G formulation activates the papillar cell population, sustaining the anagen phase and the consequent hair elongation.

Analysis of Figures 2–6 clearly shows that the Gp_4G formulation provides a general activation of dermal tissues. Although all components present in the Gp_4G formulation may collectively help to obtain this effect, the effect of antioxidant agents and red pepper extract cannot solely explain the results obtained (23,47). The key ingredient present in the Gp_4G formulation, which is Gp_4G itself, has not yet been linked to the mechanisms by

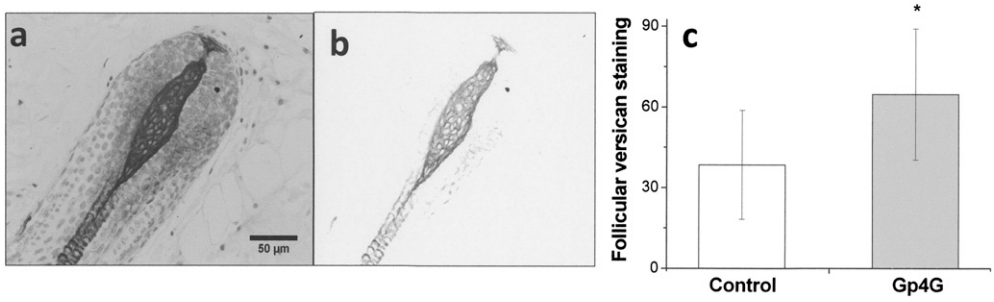

Figure 6. Effect of Gp_4G formulation on versican synthesis. (a) Immunoreaction for versican in the bulbic dorsal anagen follicles. (b) Immunoreactions after color isolation of the specific versican immunostaining. (c) Mean density (in arbitrary units) obtained in the immunocytochemical analysis for versican in the bulb dorsal follicles measured after *Image J* treatment to isolate pixels from the VER primary antibody stained.

which the compound acts in the cells and, therefore, a series of experiments was performed to propose a hypothesis for the cellular mechanism of Gp_4G.

CELLULAR MECHANISM OF Gp_4G

Experiments aiming to test the effect of Gp_4G on cellular metabolism were conducted using immortalized epithelial Hela cells and primary fibroblasts from Swiss mouse embryos. Although Gp_4G may be interacting with a variety of cell types including follicular stem cells, the aim of these studies is to provide a general intracellular activation mechanism. The other ingredients present in the Gp_4G formulation were not included in order to unveil the cellular role of Gp_4G alone. By evaluating changes in absorption in the wavelength region of nucleotide absorption, we were able to quantify the increase in the nucleotide concentrations inside cells as a function of Gp_4G concentration. Gp_4G enters Hela cells and the uptake follows a saturation plateau (Figure 7). At 6 μM (5 ppm), Gp_4G increases cell viability and the number of cell colonies by 28% and 13%, respectively (Figure 7b,c), confirming that Gp_4G stimulates Hela cells in culture. Similar, but more pronounced, results were obtained with primary fibroblasts (Figure 7d).

Gp_4G suffers asymmetric enzymatic cleavage to produce GTP and GMP in CAS (13–15, 48). Recent data showed that this conversion also happens in human cells (49). Cells have a variety of enzymes that link the total nucleoside phosphate pool with ATP-bioenergetics. For example, nucleoside diphosphate kinases, which catalyze transfer of γ-phosphate from nucleoside 5′-triphophates to nucleoside 5′-diphosphates and adenylate kinases,

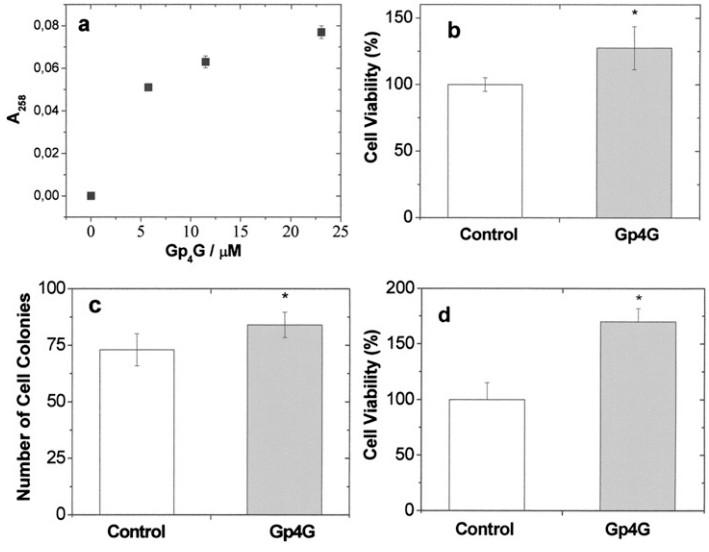

Figure 7. Gp_4G internalization in epithelial cells, viability, and colony growth. Hela cell uptake of Gp_4G. (a) Measurements were obtained by light absorption at 258 nm in Hela cells after disruption with SDS. Absorptions were discounted from control values. (b) MTT assay of cell viabilities for 10^5 Hela cells after 3-hr incubation with Gp_4G in DMEM. (c) Number of colonies of Hela cells after 8 days in growth under Gp_4G at 6μM (5 ppm). (d) MTT assay of cell viabilities for 10^5 primary fibroblast cells after 3-hr incubation with Gp_4G in DMEM. * Significantly different from controls, $p < 0.05$.

promote reversible phosphotransfer between ADP, ATP, and AMP (50). This and other enzymatic systems allow that high-energy phosphates from a triphosphate nucleoside (GTP, for instance) gets transferred to a diphosphate nucleoside (ADP, for instance), which explains the increase in ATP concentration. Quantification of intracellular ATP was conducted using the luciferin/luciferase method (25). In the cells treated with Gp_4G, there was a 38% increase in ATP concentration (Figure 8a). This increase in intracellular ATP concentration is equivalent to that observed in *Artemia salina* (14). Increase in intracellular ATP with increases in ATP/ADP ratios are know to trigger several signaling pathways that lead mainly to inhibitory metabolic regulation (respiratory control), which are not compatible with the data on cell viability and tissue activation (51,52).

Besides ATP, the asymmetric cleavage of Gp_4G and consequent catalyzed phosphotransfer systems produces di/monophosphate nucleosides, which are known to regulate several metabolic pathways, including activation of phosphofrutokinase, inhibition of ATPase, stimulation of respiration, and regulation of different types of UCPs (48–55). This could explain the cellular activation that triggers the effect on the dermal tissues shown above. Therefore, it is necessary to quantify if Gp_4G treatment would also increase the concentration of di/monophosphate nucleosides. Quantification of the intracellular concentration of nucleotides in Hela cells was conducted using HPLC (Figure 8b). Note that the treatment with Gp_4G causes an increase in the intracellular concentration of all di/monophospate nucleosides, with statistically significant differences for GDP (Figure 8). Parallel increases in concentrations of triphosphates and di/monophosphate nucleosides are not common in nature, because these nucleotides are mutually controlled and the increase in ATP concentration usually occurs with the consecutive decrease in the concentrations of ADP and AMP (50). Therefore, the treatment with Gp_4G generates a new homeostatic balance in cells, in which the concentration of both triphosphates and di/monophosphate nucleosides are increased. This new equilibrium of tri/di/monophosphate nucleoside concentration may have direct (described above) and indirect effects in cell metabolism. One example of the indirect effect would be the activation of K^+ channels, which are known to respond to the intracellular concentration of ADP/GDP (56) that activates tissue vascularization. The degree in which particular compounds are able to regulate the opening of K^+ channel varies with the tissue type. The relationship between the opening of K^+ channels and hair growth has been evidenced as the main action mechanism of minoxidil.

We propose that for Gp_4G, the activation profile observed in dermal tissues and the induction of hair growth are triggered by changes in intracellular equilibrium concentrations

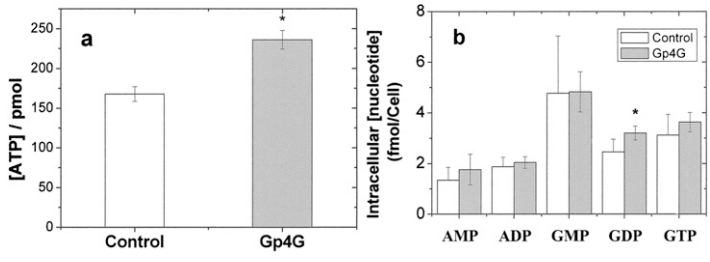

Figure 8. Intracellular nucleotide concentrations. (a) Intracellular ATP levels measured in Hela cells by the lucipherin-lucipherase protocol after 3-hr incubation with Gp_4G at 6 μM (5 ppm) cell disruption with $HClO_4$ and adjusted pH in 10^5 cells. (b) Intracellular nucleotides extracted from Hela cells and quantified by HPLC as intracellular concentration/cell.

of nucleotides in the cells in which Gp_4G enters. This metabolic activation would be independent of the cell type, which can explain the generic stimulation profile observed. Similar effects were observed by Loef and co-workers in potato tubers by providing an overdose of adenine to cause an increase in the overall size of the nucleotide pool (53). They observed parallel increases of ATP and ADP, with regulation characteristic of both ATP increases (stimulus of ADPGlc pyrophosphorylase, leading to a higher rate of starch synthesis) and ADP increases (stimulation of respiration and a decline in glycerate-3-phosphate).

Another effect that may be relevant in this process is extracellular hydrolysis of Gp_4G, releasing ATP and other nucleotides in the skin tissues, which may stimulate P2 receptors. P2 receptors are expressed in the basal and differentiated layers, especially in keratinocytes, and have been shown to be involved in the regulation of proliferation, differentiation, and apoptosis (57). This hypothesis will be tested in future investigations.

CONCLUSIONS

Gp_4G formulation has a number of biological effects on the skin, such as hair growth, angiogenesis, fibroblast activation, simulation of collagen, and versican synthesis and deposition. In cell culture, Gp_4G promotes an increase in cell viability parallel to an increase in intracellular tri- di-, and monophosphate nucleosides. Therefore, the Gp_4G formulation may lead to several structure adaptations in the epidermis that could be useful for cosmetic applications.

REFERENCES

(1) K. S. Stenn and R. Paus, Control of hair follicle cycling, *Physiol. Rev.,* **81,** 449–494 (2001).
(2) S. Muller-Rover, B. Handjiski, C. van der Veen, S. Eichmüller, K. Foitzik, I. A. McKay, K. S. Stenn, and R. Paus, A comprehensive guide for the accurate classification of murine hair follicles in distinct hair cycle stages, *J. Invest. Dermatol.,* **117,** 3–15 (2001).
(3) N. V. Botchakareva, G. Ahluwalia, and D. Shander, Apoptosis in the hair follicle, *J. Invest. Dermatol.,* **126,** 258–264 (2006).
(4) A. A. Panteleyev, C. A. B. Jahoda, and A. M. Christiano, Hair follicle predetermination, *J. Cell. Sci.,* **114**(19), 3419–3431 (2001).
(5) K. S. Stenn and R. Paus, Controls of hair follicle cyling, *Physiol. Rev.,* **81**(1), 449–494 (2001).
(6) M. Robinson, A. J. Reynolds, A. Gharzi, and C. A. B. Jahoda, *In vivo* induction of hair growth by dermal cells isolated from hair follicles after extended organ culture, *J. Invest. Dermatol.,* **117,** 596–604 (2001).
(7) N. Adhirajan, T. R. Kumar, N. Shanmugasundaram, and M. Babu, *In vivo* and *in vitro* evaluation of hair growth potential of *Hibiscus rosa-sinensis* Linn, *J. Ethnopharm.,* **88,** 235–239 (2003).
(8) R. Rizzuto, The collagen-mitochondira connection, *Nat. Genet.,* **35**(4), 300–301 (2003).
(9) Y. Tjusi, S. Denda, T. Soma, L. Raftery, T. Momoi, and T. Hibino, A potential suppressor of TGF-β delays catagen progression in hair follicles, *J. Invest. Dermatol.,* **8,** 65–68 (2003).
(10) M. Lino, R. Ehama, T. Iwabuchi, Y. Nakazawa, R. Ideta, Y. Tsuji, T. Okumura, Y. Watanabe, H. Oura, H. Arase, and J. Kishimoto, "Adenosine," a novel hair-growth promoting biomolecule: Its molecular mechanism of action and efficacy, *25th IFSCC Conference, Barcelona,* 91–96 (2008).
(11) S. Murad, L. C. Walker, S. Tajima, and S. R. Pinell, Minimal structural requirements for minoxidil inhibition of lysyl hydroxilase in cultured fibroblasts, *Arch. Biochem. Biophys.,* **308**(1), 42–47 (1994).
(12) D. van Mater, F. T. Kolligs, A. A. Dlugosz, and E. R. Fearon, Transient activation of β-catenin signaling in cutaneous keratinocytes is sufficient to trigger the active growth phase of the hair cycle in mice, *Genes Develop.,* **17,** 1219–1224 (2003).
(13) F. J. Finamore and A. H. Warner, The occurrence of p^1,p^4-diguanosine 5′-tetraphosphate in brine shrimp eggs, *J. Biol. Chem.,* **238,** 344–348 (1963).

(14) A. H. Warner and F. J. Finamore, Isolation purification and characterization of p^1 p^4-diguanosine 5′-tetraphosphate asymmetrical-pyrophosphohydrolase from brine shrimp eggs, *Biochem.,* 4(8), 1568–1575 (1965).
(15) A. H. Warner and J. S. Clegg, Diguanoside nucleotide metabolism and the survival of *Artemia* empryos during years of continuous anoxia, *Eur. J. Biochem.,* **268,** 1568–1576 (2001).
(16) E. Rapaport and P. C. Zamecnik, Presence of diadenosine 5′,5‴-p^1,p^4-tetraphosphate (Ap_4A) in mammalian cells in levels varying widely with proliferative activity of the tiassue: A possible positive "pleiotypic activator," *Proc. Natl. Acad. Sci. USA,* **73**(11), 3984–3988 (1976).
(17) L. Fort-Lacoste and M. Jeanjean, Association de diguanoside tetraphosphateet de derivés nicotiniques, destinées aux traitement des desódres capillaries, notamment pour lutter contre la chute de cheveux, *Eur. Pat. Office,* EP 1 336 402 A1 (2003).
(18) N. Kocever, I. Glavac, R. Injac, and S. Kreft, Comparison of capillary electrophoresis and high performance liquid chromatography for determination of flavonoids in *Achillea millefolium, J. Pharm. Biom. Anal.,* **46,** 609–614 (2008).
(19) N. Nenadis, O. Lazaridou, and M. Z. Tsimidou, Use of reference compounds in antioxidant activity assessment, *J. Agric. Food. Chem.,* **55,** 5452–5460 (2007).
(20) D. Huang, B. Ou, and R. L. Prior, The chemistry behind antioxidant capacity assays, *J. Agric. Food Chem.,* **53,** 1841–1856 (2005).
(21) P. J. Tsai, J. Mcintosh, P. Pearce, B. Camden, and B. R. Jorden, Anthocyanin and antioxidant capacity in Roselle (*Hibiscus Sabdarifa* L.) extract, *Food Res. Int.,* **35,** 351–356 (2002).
(22) Y. Milner, J. Sudnik, M. Filippi, M. Kizoulis, M. Kashgarin, and K. Stenn, Exogen, shedding phase of the hair growth cycle: Characterization of a mouse model, *J. Invest. Dermatol.,* **119,** 639–644 (2002).
(23) D. Rival, S. Bonnet, B. Shom, and E. Perrier, A Hibiscus abelmoschus seed extract as a protective active ingredient to favore FGF-2 activity in skin, *Int. J. Cosmet. Sci.,* **31,** 419–426 (2009).
(24) J. T. Headington, Transverse microscopic anatomy of the human scalp: A basis for a morphometric approach to disorders of the hair follicle, *Arch. Dermatol.,* **120,** 449–456 (1984).
(25) M. Lehtokari, P. Nikkola, and J. Paatero, Determination of ATP from compost using the firefly bioluminescence technique, *Eur. J. Appl. Microbiol. Biotechol.,* **17,** 187–190 (1983).
(26) H. D. Dellman and J. A. Eurell, *Textbook of Veterinary Histology, 5th Ed.* (Williams and Wilkins, Baltimore, 1998), Ch. 3,6.
(27) D. Oh, Validating proteins as functional cosmetic ingredients—An hGH case, *SOFW-J, Int. J. App. Sci.,* **135,** 2–14 (2009).
(28) P. Kaur, Interfollicular stem cells: Identification, challenges, potential, *J. Invest. Dermatol.,* **126,** 1450–1458 (2006).
(29) G. Cotsarelis, Epithelial stem cells: A folliculocentric view, *J. Invest. Dermatol.,* **126,** 1459–1468 (2006).
(30) L. Alonso and E. Fuchs, Stem cells of the skin epithelium, *Proc. Natl. Acad. Sci. USA,* **100,** 11830–11835 (2003).
(31) H. Cho, H. Lee, E. Kim, K. Park, M. Chang, J. Kim, C. Lee, and D. Oh, Analysis of the effects of hGH using living skin equivalents, *Tiss. Eng. Regener. Med.,* 4, 406–410 (2007).
(32) D. L. du Cros, R. G. LeBaron, and J. R. Couchman, Association of versican with dermal matrices and its potential role in hair follicle development and cycling, *J. Invest. Dermatol.,* **105**(3), 426–431 (1995).
(33) L. C. Junqueira, G. S. Montes, J. E. Martins, and P. P. Joazeiro, Dermal collagen distribution: A histochemical and ultrastructural study, *Histochem.,* **79,** 397–403 (1983).
(34) T. Kukita, K. Hata, A. Kukita, and T. Iijima, Laminin, a major basement membrane component of the blood vessel, as a negative regulator of osteoclastogenesis, *Calcif. Tiss. Int.,* **63,** 140–142 (1998).
(35) F. Tuckett and G. M. Morriss-Kay, The distribution of fibronectin, laminin and entactinin in the neurulating rat embryo studied by indirect immunofluorescence, *Embryol. Exp. Morph.,* **94,** 95–112 (1986).
(36) M. G. Kinsella, S. L. Bressler, and T. N. Wight, The regulated synthesis of versican, decorin, and biglycan: Extracellular matrix proteoglycans that influence cellular phenotype, *Crit. Rev. Eukaryot. Gene Expr.,* 14(3), 203–234 (2004).
(37) T. N. Wight, Versican: A versatile extracellular matrix proteoglycan in cell biology, *Curr. Opin. Cell. Biol.,* 14, 617–623 (2002).
(38) T. Soma, M. Tajima, and J. Kishimoto, Hair cycle-specific expression of versican in human hair follicles, *J. Dermatol. Sci.,* **39,** 147–154 (2005).
(39) B. P. Toole, Hyaluronan is not just a good! *J. Clin. Invest.,* **106**(3), 335–336 (2000).

(40) B. P. Toole, "Glycosaminoglycans in Morphogenesis," in *Cell Biology of Extracellular Matrix.,* E. D. Hay, Ed. (Plenum Press. New York, 1981), pp 259–294.
(41) W. Sheng, G. Wang, D. P. La Pierre, J. Wen, Z. Deng, C. K. Wong, D. Y. Lee, and B. B. Yang, Versican mediates mesenchymal–epithelial transition, *Mol. Biol. Cell.,* **17**(4), 2009–2020 (2006).
(42) S. San Martin, M. Soto-Suazo, and T.M.T. Zorn, Distribution of versican and hyaluronan in the mouse uterus during decidualization, *Braz. J. Med. Bio. Res.,* **36:** 879X (2003).
(43) R. M. Salgado, L. P. Capelo, R. R. Favaro, J. D. Glazier, J. D. Aplin, and T. M. Zorn, Hormone-regulated expression and distribution of versican in mouse uterine tissues, *Reprod. Biol. Endocrinol.,* **7**(1), 60 (2009).
(44) J. Kishimoto, R. Ehama, L. Wu, S. Jiang, N. Jiang, and R. Burgenson, Selective activation of the versican promoter by epithelial–mesenchymal interactions during hair follicle development, *Proc. Natl. Acad. Sci. USA,* **96,** 7336–7341 (1999).
(45) J. R. Couchman, J. L. King, and K. J. McCarthy, Distribution of two basement membrane proteoglycans through hair follicle development and the hair growth cycle in the rat, *J. Invest. Dermatol.,* **94,** 65–70 (1990).
(46) J. R. Couchman, K. J. McCarthy, and A. Woods, Proteoglycans and glycoproteins in hair follicle development and cycling, *Ann. N. Y. Acad. Sci.,* **642,** 243–251 (1991).
(47) E. Bodó, T. Bíró, A. Telek, G. Czifra, Z. Griger, B. I. Tóth, A. Mescalchin, T. Ito, A. Bettermann, L. Kovács, and R. Paus, A hot new twist to hair biology: Involvment of vanilloid receptor-1 (VR1/TRPV1) signaling in human hair growth control, *Am. J. Pathol.,* **166,** 985–998 (2005).
(48) M. F. Renart, J. Renart, M. G. Sillero, and A. Sillero, Guanosine monophosphate reductase from *Artemia salina:* Inhibition by xanthosine monophosphate and activation by diguanosine tetraphosphate, *Biochemistry,* **15**(23), 4962–4966 (1976).
(49) P. Vollmayer, T. Clair, J. W. Goding, K. Sano, J. Servos, and H. Zimmermann, Hydrolysis of diadenosine polyphosphates by nucleotide pyrophosphatases/phosphodi-esterases, *Eur. J. Biochem.,* **270,** 2971–2978 (2003).
(50) P. P. Dzeja and A. Terzic, Phosphotransfer networks and cellular energetic, *J. Exp. Biol.,* **206,** 2039–2047 (2003).
(51) B. Ludwig, E. Bender, S. Arnold, M. Hüttemann, I. Lee, and B. Kadenbach, Cytochrome c oxidase and the regulation of oxidative physphorylation, *Chem. Biochem.,* **2**(6), 392–403 (2001).
(52) C. S. Henry, L. J. Broadbelt, and V. Hatzimanikatis, Thermodynamics-based metabolic flux analysis, *Biophys. J.,* **92,** 1792–1805 (2007).
(53) I. Loef, M. Stitt, and P. Geigenberger, Increased levels of adenine nucleotides modify the interaction between starch synthesis and respiration when adenine is supplied to discs from growing potato tubers, *Planta,* **212,** 782–791 (2001).
(54) S. Thomas, and D. A. Fell, A control analysis exploration of the role of ATP utilization in glycolytic-flux control and glycolytic-metabolite-concentration regulation, *Eur. J. Biochem.,* **258,** 956–967 (1998).
(55) M. Klingenberg, Uncoupling proteins—How do they work and how are they regulated, *IUBMB Life,* **52,** 175–179 (2001).
(56) A. P. Babenko, G. Gonzalez, L. Aguilar-Bryan, and J. Bryan, Reconstituted human cardiac KATP channels: Functional identity with the native channels from the sarcolemma of human ventricular cells, *Circ. Res.,* **83**(11), 1132–1143(1998).
(57) H. E. Burrel, B. Wlodarski, B. J. Foster, K. A. Buckley, G. R. Sharpe, J. M. Quayle, A. W. M. Simpson, and J. A. Gallagher, Human keratinocytes release ATP and utilize three mechanisms for nucleotide intercorversion at the cell surface, *J. Biol. Chem.,* **280,** 29667–29676 (2005).